

Global dynamics of coupled standard maps

T. Manos^{1,2}, Ch. Skokos³ and T. Bountis¹

¹ Center for Research and Applications of Nonlinear Systems (CRANS),
Department of Mathematics, University of Patras, GR-26500, Greece.
`thanosm@master.math.upatras.gr`, `bountis@math.upatras.gr`

² Observatoire Astronomique de Marseille-Provence (OAMP), 2 Place Le Verrier,
F-13248 Marseille, Cédex 04, France.

³ Astronomie et Systèmes Dynamiques, IMCCE, Observatoire de Paris,
77 Av. Denfert-Rochereau, F-75014, Paris, France. `hskokos@imcce.fr`

Summary. Understanding the dynamics of multi-dimensional conservative dynamical systems (Hamiltonian flows or symplectic maps) is a fundamental issue of nonlinear science. The Generalized ALignment Index (GALI), which was recently introduced and applied successfully for the distinction between regular and chaotic motion in Hamiltonian systems [1], is an ideal tool for this purpose. In the present paper we make a first step towards the dynamical study of multi-dimensional maps, by obtaining some interesting results for a 4-dimensional (4D) symplectic map consisting of $N = 2$ coupled standard maps [2]. In particular, using the new GALI₃ and GALI₄ indices, we compute the percentages of regular and chaotic motion of the map equally reliably but much faster than previously used indices, like GALI₂ (known in the literature as SALI).

1 Definition and behavior of GALI

Let us first briefly recall the definition of GALI and its behavior for regular and chaotic motion, adjusting the results obtained in [1] to symplectic maps. Considering of a $2N$ -dimensional map, we follow the evolution of an orbit (using the equations of the map) together with k initially linearly independent deviation vectors of this orbit $\vec{\nu}_1, \vec{\nu}_2, \dots, \vec{\nu}_k$ with $2 \leq k \leq 2N$ (using the equations of the tangent map). The Generalized Alignment Index of order k is defined as the norm of the wedge or exterior product of the k unit deviation vectors:

$$GALI_k(i) = \| \hat{\nu}_1(i) \wedge \hat{\nu}_2(i) \wedge \dots \wedge \hat{\nu}_k(i) \| \quad (1)$$

and corresponds to the volume of the generalized parallelepiped, whose edges are these k vectors. We note that the hat ($\hat{\cdot}$) over a vector denotes that it is of unit magnitude and that i is the discrete time.

In the case of a chaotic orbit all deviation vectors tend to become linearly dependent, aligning in the direction of the eigenvector which corresponds to the maximal Lyapunov exponent and $GALI_k$ tends to zero following an exponential law $\sim e^{-[(\sigma_1 - \sigma_2) + (\sigma_1 - \sigma_3) + \dots + (\sigma_1 - \sigma_k)]i}$, where $\sigma_1, \dots, \sigma_k$ are approx-

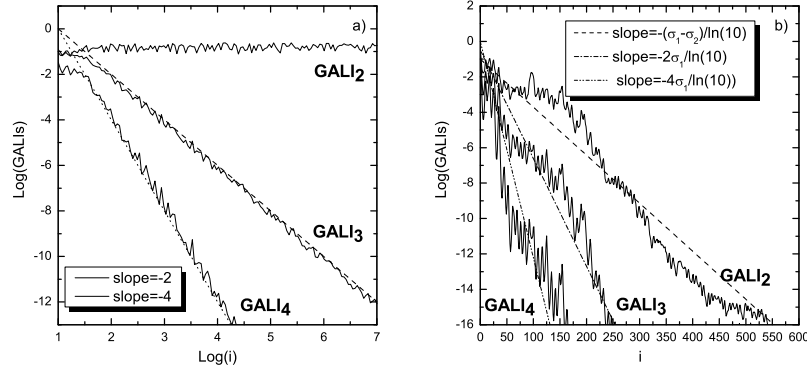


Fig. 1. The evolution of $GALI_k$, $k = 2, 3, 4$, with respect to the number of iterations i for a) the regular orbit R and b) the chaotic orbit C. The plotted lines correspond to functions proportional to n^{-2} , n^{-4} in a) and to $e^{-(\sigma_1 - \sigma_2)i}$, $e^{-2\sigma_1 i}$, $e^{-4\sigma_1 i}$ for $\sigma_1 = 0.070$, $\sigma_2 = 0.008$ in b).

imations of the first k largest Lyapunov exponents. In the case of regular motion on the other hand, all deviation vectors tend to fall on the N -dimensional tangent space of the torus on which the motion lies. Thus, if we start with $k \leq N$ general deviation vectors they will remain linearly independent on the N -dimensional tangent space of the torus, since there is no particular reason for them to become aligned. As a consequence $GALI_k$ remains practically constant for $k \leq N$. On the other hand, $GALI_k$ tends to zero for $k > N$, since some deviation vectors will eventually become linearly dependent, following a particular power law, i. e. $GALI_k(i) \sim i^{2(N-k)}$.

2 Dynamical study of a 4D standard map

As a model for our study we consider the 4D symplectic map:

$$\begin{aligned} x'_1 &= x_1 + x'_2 & x'_2 &= x_2 + \frac{K}{2\pi} \sin(2\pi x_1) - \frac{B}{2\pi} \sin[2\pi(x_3 - x_1)] \\ x'_3 &= x_3 + x'_4 & x'_4 &= x_4 + \frac{K}{2\pi} \sin(2\pi x_3) - \frac{B}{2\pi} \sin[2\pi(x_1 - x_3)] \end{aligned} \pmod{1}, \quad (2)$$

which consists of two coupled standard maps [2] and is a typical nonlinear system, in which regions of chaotic and regular dynamics are found to coexist. In our study we fix the parameters of the map (2) to $K = 0.5$ and $B = 0.05$.

In Fig. 1, we show the behavior of GALIs for two different orbits: a regular orbit R with initial conditions $(x_1, x_2, x_3, x_4) = (0.55, 0.10, 0.54, 0.01)$ (Fig. 1a), and a chaotic orbit C with initial conditions $(x_1, x_2, x_3, x_4) = (0.55, 0.10, 0.005, 0.01)$ (Fig. 1b). The positive Lyapunov exponents of orbit C were found to be $\sigma_1 \approx 0.070$, $\sigma_2 \approx 0.008$. From the results of Fig. 1 we see that the evolution of GALIs is described very well by the theoretically obtained approximations presented in Sect. 1.

Let us now turn our attention to the study of the global dynamics of map (2). From the results Fig. 1 we conclude that in the case of 4D maps,

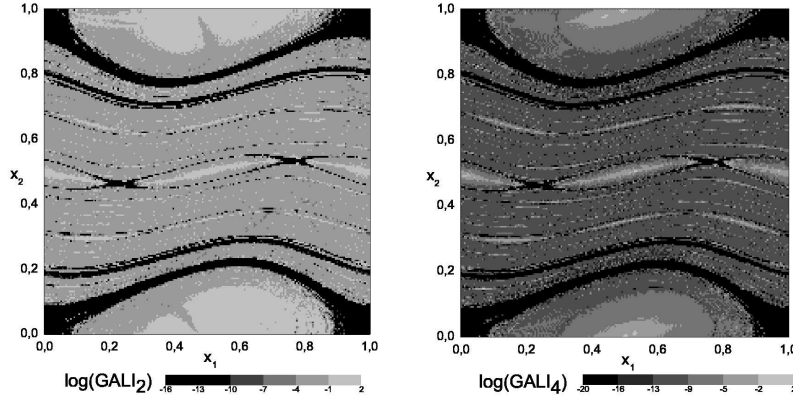


Fig. 2. Regions of different values of the GALI_2 (left panel) and GALI_4 (right panel) for a grid of 500×500 initial conditions on the subspace $x_3 = 0.54$, $x_4 = 0.01$ of map (2) for $K = 0.5$ and $B = 0.05$.

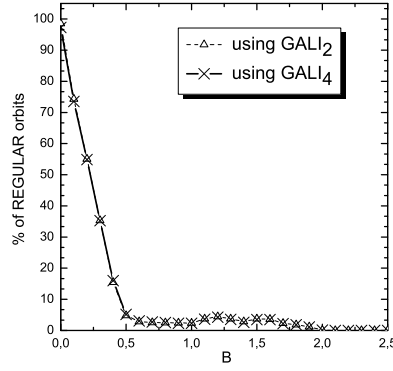


Fig. 3. Percentages of regular orbits on the subspace $x_3 = 0.54$, $x_4 = 0.01$ of map (2) for $K = 0.5$, as a function of the parameter $B \in [0, 2.5]$.

GALI_2 has different behavior for regular and chaotic orbits. In particular, GALI_2 tends exponentially to zero for chaotic orbits ($\text{GALI}_2 \sim e^{-(\sigma_1 + \sigma_2)i}$) while it fluctuates around non-zero values for regular orbits. This difference in the behavior of the index can be used to obtain a clear distinction between regular and chaotic orbits. Let us illustrate this by following up to $i = 4000$ iterations, all orbits whose initial conditions lie on a 2-dimensional grid of 500×500 equally spaced points on the subspace $x_3 = 0.54$, $x_4 = 0.01$, of the 4-dimensional phase space of the map (2), attributing to each grid point a color according to the value of GALI_2 at the end of the evolution. If GALI_2 of an orbit becomes less than 10^{-10} for $i < 4000$ the evolution of the orbit is stopped, its GALI_2 value is registered and the orbit is characterized as chaotic. The outcome of this experiment is presented in the left panel of Fig. 2.

But also $GALI_4$ can be used for discriminating regular and chaotic motion. From the theoretical predictions for the evolution of $GALI_4$, we see that after $i = 1000$ iterations the value of $GALI_4$ of a regular orbit should become of the order of 10^{-16} , since $GALI_4 \sim t^{-4}$, although the results of Fig. 1 show that more iterations are needed for this threshold to be reached, due to an initial transient time where $GALI_4$ does not decrease significantly. On the other hand, for a chaotic orbit $GALI_4$ has already reached extremely small values at $i = 1000$ due to its exponential decay ($GALI_4 \sim e^{-4\sigma_1 i}$). Thus, the global dynamics of the system can be revealed as follows: we follow the evolution of the same orbits as in the case of $GALI_2$ and register for each orbit the value of $GALI_4$ after $i = 1000$ iterations. All orbits having values of $GALI_4$ significantly smaller than 10^{-16} are characterized as chaotic, while all others are considered as non-chaotic. In the right panel of Fig. 2 we present the outcome of this procedure.

From the results of Fig. 2, we see that both procedures, using $GALI_2$ or $GALI_4$ as a chaos indicator, give the same result for the global dynamics of the system, since in both cases 16% of the orbits are characterized as chaotic. These orbits correspond to the black colored areas in both panels of Fig. 2. One important difference between the two procedures is their computational efficiency. Even though $GALI_4$ requires the computation of four deviation vectors, instead of only two that are needed for the evaluation of $GALI_2$, using $GALI_4$ we were able to get a clear dynamical ‘chart’, not only for less iterations of the map (1000 instead of 4000 needed for $GALI_2$), but also in less CPU time. In particular, for the computation of the data of the left panel of Fig. 2 (using $GALI_2$) we needed 1 hour of CPU time on an Athlon 64bit, 3.2GHz PC, while for the data of the left panel of the same figure (using $GALI_4$) only 14 minutes of CPU time were needed.

Using the above-described method, both for $GALI_2$ and $GALI_4$, we were able to compute very fast and accurately the percentages of regular motion for several values of parameter B . In Fig. 3 we plot the percentage of regular orbits for $B \in [0, 2.5]$ where B varies with a step $\delta B = 0.1$. We see that the two curves practically coincide, but using $GALI_2$ we needed almost four times more CPU time. So, it becomes evident that a well-tailored application of $GALI_k$, with $2 < k$, can significantly diminish the CPU time required for the detailed ‘charting’ of phase space regions, compared with that for $GALI_2$.

Acknowledgments

T. Manos was supported by the “Karatheodory” graduate student fellowship No B395 of the Univ. of Patras, the program “Pythagoras II” and the Marie Curie fellowship No HPMT-CT-2001-00338. Ch. Skokos was supported by the Marie Curie Intra-European Fellowship No MEIF-CT-2006-025678.

References

1. Ch. Skokos, T. Bountis and Ch. Antonopoulos, *Physica D*, **231**, 30, (2007).
2. H. Kantz and P. Grassberger, *J. Phys. A: Math. Gen.*, **21** L127, (1988).